

## Aptamer/Nanoparticle-Based Sensitive, Multiplexed Electronic Coding of Proteins and Small Biomolecules through a Backfilling Strategy

Xiaoqing Qian, Yun Xiang,\* Haixia Zhang, Ying Chen, Yaqin Chai, and Ruo Yuan\*[a]

The development of sensitive and selective bioassays capable of monitoring important biomolecules in a multiplexed fashion is a major goal in biosensing.<sup>[1–5]</sup> In many cases, measurement of a single biomarker is not sufficient to diagnose and follow the disease status. Rather, simultaneous measurement of a panel of biomarkers is necessary to reach this goal; this has led to increasing research on multiplexed analysis of biomolecules. Various multiplexed detection schemes for DNA or proteins based on labels with distinct readouts, such as optically<sup>[6–11]</sup> or electrochemically<sup>[12–15]</sup> encoded quantum dots, multisegment nanowires,<sup>[16–19]</sup> dye-embedded microspheres,<sup>[20–24]</sup> and biobarcode nanoparticles,<sup>[25,26]</sup> have thus been demonstrated.

Although multiplexed analysis of DNA or proteins is well developed, simultaneous monitoring of analytes with significant difference in sizes, for instance, small biomolecules and proteins, has rarely been exploited and remains a challenge mainly due to the lack of double-probe sandwich assay formats for the low-molecular-weight analytes.

Herein, we report, for the first time, a novel aptamer/nanoparticle-based backfilling strategy for one-spot simultaneous detection of proteins and small biomolecules, employing lysozyme and adenosine triphosphate (ATP) as the model target analytes. Our approach relies on target-induced release of aptamers from the DNA duplexes on a sensing surface, followed by backfilling hybridization of the resulting single-stranded DNA molecules with aptamers conjugated to the electrochemically encoded nanoparticles. Subsequent unique electrochemical (EC) signatures of the acid-dissolved nanoparticles at distinct potential positions with well-resolved peaks thus reflect the identities and concentrations of lysozyme and ATP. Compared with previously

reported multiplexed detection schemes, our new analysis route for proteins and small biomolecules offers three clear advantages. First, simultaneous determination of biomolecules with distinct molecular weights (lysozyme, 14.3 kDa versus ATP, 507.2 Da) is achieved for the first time with electrochemically encoded nanoparticle tags. Second, in contrast to other common “signal off” assay formats for lysozyme<sup>[27–29]</sup> and ATP based on target-induced displacement<sup>[30–32]</sup> or conformational changes of the corresponding aptamers,<sup>[33–36]</sup> our multiplexed method is a “signal on” configuration, which exhibits improved sensitivity.<sup>[35]</sup> Third, the analytical signal amplification by the nanoparticle labels composed of a large number of metal ions and the high sensitivity of the voltammetric stripping detection lead to low-concentration determination of the target analytes. The combination of these advantages facilitates the detection of biomolecules with distinct sizes in a multiplexed and sensitive manner.

Our multiplexed analysis approach for proteins and small molecules based on the aptamer/nanoparticle bioconjugates and the backfilling strategy, illustrated in Figure 1, involves the formation of a mixed self-assembled monolayer of thiol-modified cDNA/aptamer duplexes and 6-mercapto-1-hexanol blocking on a gold substrate, release of the aptamer/target complexes from the surface upon the addition of the targets, backfilling hybridizations of the single-stranded, thiol-modified cDNAs on the gold substrate with the aptamer/nanoparticle bioconjugates, and square-wave voltammetric (SWV) stripping measurement of the Pb<sup>II</sup> and Cd<sup>II</sup> ions released upon acid dissolution of the nanoparticle tags (PbS and CdS). The EC signatures of the released ions exhibit well-resolved peaks (PbS, –0.55 V; CdS, –0.71 V) with positions and sizes indicative of the identities and concentrations of the target analytes, lysozyme and ATP, respectively. During the assay, the addition of higher concentrations of the targets leads to the removal of more aptamers from the gold surface and formation of more single-stranded, thiol-modified cDNAs available for backfilling hybridization with the aptamer/nanoparticle bioconjugates. Larger voltammet-

[a] X. Q. Qian, Prof. Y. Xiang, H. X. Zhang, Y. Chen, Prof. Y. Q. Chai, Prof. R. Yuan  
Key Laboratory on Luminescence and Real-Time Analysis  
Ministry of Education  
School of Chemistry and Chemical Engineering  
Southwest University, Chongqing 400715 (P.R. China)  
Fax: (+86) 68254000  
E-mail: yunatswu@swu.edu.cn  
yuanruo@swu.edu.cn

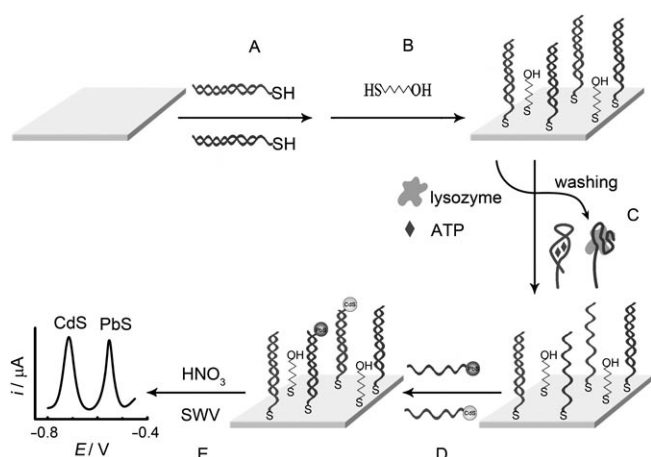


Figure 1. Schematic illustration of the aptamer/nanoparticle-based backfilling protocol for one-spot simultaneous electronic detection of lysozyme and ATP. A) Coassembly of thiol-modified cDNA/aptamer duplexes on a gold substrate, B) blocking of the gold surface with 6-mercapto-1-hexanol, C) addition of the target analytes lysozyme and ATP, D) incubation with aptamer/nanoparticle bioconjugates, E) acid dissolution of the nanoparticle tags (PbS and CdS) and EC measurement of the Pb<sup>II</sup> and Cd<sup>II</sup> ions released from the nanoparticles.

ric stripping peaks from the Pb<sup>II</sup> and Cd<sup>II</sup> ions are then expected.

We first evaluated our backfilling strategy for single-analyte determination by immobilizing SH-cDNA/aptamer duplexes for lysozyme on the gold surface. As displayed in Figure 2A, the presence of lysozyme leads to a sharp increase of the voltammetric stripping peak of Pb<sup>II</sup> compared with that in the absence of lysozyme (Figure 2Ai), which reflects the release of the surface-hybridized, lysozyme-binding aptamer and successful hybridization of the aptamer/PbS with the corresponding cDNA. Meanwhile, as the concentration of lysozyme increases, more PbS nanoparticles are captured on the surface and an increasing stripping current of Pb<sup>II</sup> is observed. The stripping current of Pb<sup>II</sup> thus shows a concentration dependence on the lysozyme concentration from 0.2 to 100 nM (Figure 2B). The calibration curve of the stripping current of Pb<sup>II</sup> versus  $c_{\text{lysozyme}}$  is shown in the inset of Figure 2B; this indi-

cates a linear relationship over the 0.2–10 nM range. The detection limit for lysozyme is estimated to be 0.12 nM, based on the signal-to-noise ratio of 3.

Similarly, this aptamer/nanoparticle-based backfilling strategy was also applied to detect ATP with CdS nanoparticles as labels. The size of the voltammetric stripping peak of Cd<sup>II</sup> from the CdS nanoparticle tags is dependent on the concentration of ATP (Figure 2C). The corresponding calibration curve (inset in Figure 2D) for ATP detection indicates a linear relationship over the 0.01–10  $\mu\text{M}$  range, and a detection limit of 4.8 nM could be derived. Such low detection limits for lysozyme and ATP detections based on the nanoparticle labels and the backfilling strategy could be ascribed to two facts. First, instead of the universal target-induced displacement or conformational change “signal off” configuration, our protocol is a “signal on” detection format, which means that the presence of even low levels of target analyte result in a stripping peak of the nanoparticle labels. Besides, the “signal on” detection scheme has shown improved sensitivity over the “signal off” one.<sup>[37]</sup> Second, acid dissolution of the nanoparticle labels releases a large number of metal ions to be monitored electrochemically, which act as signal amplifications for target-analyte detection. Moreover, SWV stripping is demonstrated to be an ul-

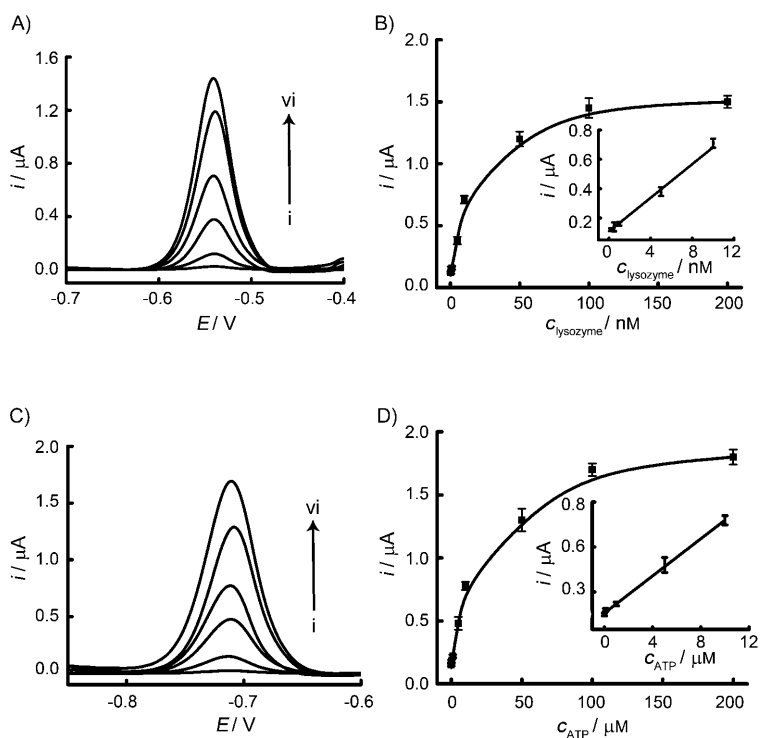


Figure 2. A) SWVs for increasing concentrations of lysozyme: i) 0, ii) 0.2, iii) 5, iv) 10, v) 50, and vi) 100 nM. B) Current response of Pb<sup>II</sup> versus  $c_{\text{lysozyme}}$  over the 0.2–200 nM range. Inset: the calibration curve for lysozyme detection over the 0.2–10 nM range. C) SWVs for increasing concentrations of ATP: i) 0, ii) 0.01, iii) 5, iv) 10, v) 50, and vi) 100  $\mu\text{M}$ . D) Current response of Cd<sup>II</sup> versus  $c_{\text{ATP}}$  over the 0.01–200  $\mu\text{M}$  range. Inset: the calibration curve for ATP detection over the 0.01–10  $\mu\text{M}$  range. SWV measurements were carried out in 0.2 M acetate buffer (10 ppm Hg<sup>II</sup>, pH 5.2) with 1 min pretreatment at +0.6 V, 2 min accumulation at −1.1 V, and scanning of the potential from −1.0 to −0.3 V with a potential step of 4 mV, a frequency of 25 Hz, and an amplitude of 25 mV. The error bars represent the standard deviations of three parallel tests.

trasensitive technique for monitoring metal ions, such as  $\text{Cd}^{\text{II}}$ ,  $\text{Pb}^{\text{II}}$ ,  $\text{Zn}^{\text{II}}$ , and  $\text{Hg}^{\text{II}}$ . The coupling of the “built in” amplification nature of nanoparticles by the metal ions and the high sensitivity of SWV thus leads to sensitive detection of lysozyme and ATP.

The selectivity of our assay protocol was investigated against other control molecules, and we found that the specific target analyte led to a substantial increase in the stripping current of the corresponding nanoparticle labels, whereas the control molecules showed minimal increase. As evidenced by Figure 3A and B, despite the existence of a large excess (100-fold) of the control molecules, thrombin

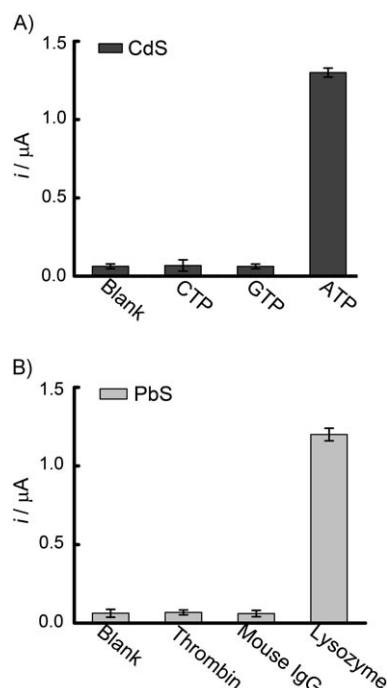


Figure 3. Specificity investigations against nontarget molecules: A) ATP (50  $\mu\text{M}$ ) versus GTP (5 mM) and CTP (5 mM). B) lysozyme (50 nM) versus thrombin (5  $\mu\text{M}$ ) and mouse IgG (5  $\mu\text{M}$ ).

(5  $\mu\text{M}$ ) and mouse IgG (5  $\mu\text{M}$ ) for lysozyme (50 nM), or cytidine triphosphate (CTP, 5 mM) and guanosine triphosphate (GTP, 5 mM) for ATP (50  $\mu\text{M}$ ), no significant stripping current increases of the corresponding nanoparticles are observed compared with the blank tests (0 nM target). However, the presence of a small amount of lysozyme or ATP results in dramatic stripping current increases of  $\text{Pb}^{\text{II}}$  and  $\text{Cd}^{\text{II}}$ , respectively, suggesting the high specificity of our assay.

Besides the sensitive and selective analysis of lysozyme and ATP separately, we implemented our strategy for multiplexed detection of these two target analytes. Figure 4B shows that the addition of lysozyme (10 nM) alone leads to an apparent stripping peak of  $\text{Pb}^{\text{II}}$ , but not of  $\text{Cd}^{\text{II}}$ . The addition of ATP (10  $\mu\text{M}$ ) performs similarly with the increase of the stripping peak of  $\text{Cd}^{\text{II}}$  but not of  $\text{Pb}^{\text{II}}$  (Figure 4C), which indicates a minimal cross reactivity for the different targets.

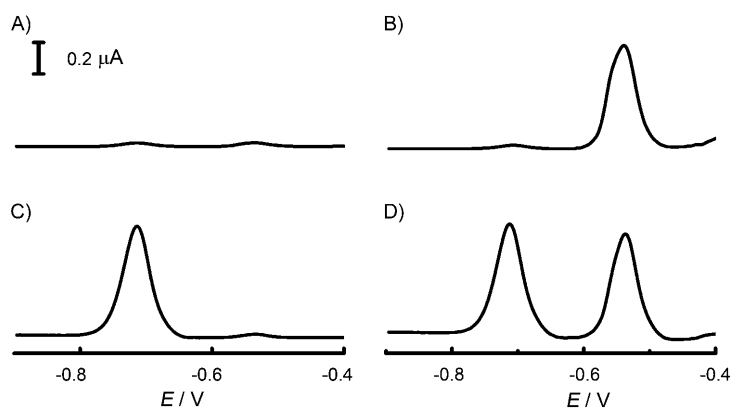


Figure 4. SWVs for the presence of A) 0  $\mu\text{M}$  lysozyme and 0  $\mu\text{M}$  ATP, B) 10 nM lysozyme, C) 10  $\mu\text{M}$  ATP and, D) 10 nM lysozyme and 10  $\mu\text{M}$  ATP in the testing buffer.

More importantly, the presence of both lysozyme and ATP leads to significant increases of both stripping peaks (Figure 4D), suggesting the capability of our assay protocol for one-spot simultaneous detection of multiple target analytes. A series of six repetitive measurements of a mixture containing 10 nM lysozyme and 10  $\mu\text{M}$  ATP yielded reproducible  $\text{Pb}^{\text{II}}$  and  $\text{Cd}^{\text{II}}$  peaks, respectively, with relative standard deviations of 6.6 and 8.2 %.

In summary, we have demonstrated a sensitive, selective, and multiplexed assay protocol for simultaneous monitoring of proteins and small molecules based on the electrochemically encoded nanoparticle labels and the backfilling strategy. The unique EC stripping patterns of the nanoparticle labels enable simultaneous monitoring of multiple analytes in one single run, whereas the “signal on” assay format and the dramatic signal amplification by the nanoparticle labels as well as the high sensitivity of the SWV technique offer low-level determination of the target analytes. Considering the wide stripping potential window for different metal ions, this strategy can be expanded to simultaneous detection of up to six different analytes in a single run by the selection of various nanoparticles labels (e.g.,  $\text{ZnS}$ :  $-1.1$  V and  $\text{GaAs}$ :  $-0.9$  V). Further amplification could be achieved by encapsulating multiple nanoparticles in polymeric microbeads as tags.<sup>[38,39]</sup> Our aptamer/nanoparticle-based backfilling strategy thus opens new opportunities for multiplexed clinical diagnosis of different molecules with distinct sizes.

## Experimental Section

**Materials:** Sodium bis(2-ethylhexyl)sulfosuccinate (AOT), cysteamine hydrochloride, 2-mercaptoethane sulfonate, lysozyme, thrombin, mouse IgG, and 6-mercapto-1-hexanol were purchased from Sigma (St. Louis, MO). Sodium chloride,  $\text{Cd}(\text{NO}_3)_2$ ,  $\text{Pb}(\text{NO}_3)_2$ ,  $\text{Na}_2\text{S}$ , pyridine, hexane, sodium acetate, acetic acid, acetone, and methanol were purchased from Kelong Chemical (Chengdu, China).  $\text{Hg}^{\text{II}}$  standard solution was received from the Chinese CRM/CM Information Center (Beijing, China). ATP, CTP, and GTP were bought from Worthington Biochemical (Lakewood, NJ, USA). The lysozyme (LBA)- and ATP (ABA)-binding aptamers and

the corresponding complementary SH-cDNAs were ordered from Shanghai Sangon Biological Engineering Technology and Services (Shanghai, China) with the sequences as follows: LBA: 5'-ATCTACGAATTCATCAGGGCTAAAGAGTGCAGAGTTACTTAG-3'; SH-LBA: 5'-ATCTACGAATTCATCAGGGCTAA, AGAGTGCAGAGTTACTTAG-(CH<sub>2</sub>)<sub>6</sub>-SH-3'; SH-cDNA<sub>1</sub>: 5'-CCTGATGAATTCGTAGATACACTG-(CH<sub>2</sub>)<sub>6</sub>-SH-3'; ABA: 5'-ACCTGGGGGAGTATTGCGGAGGAAGGT-3'; SH-ABA: 5'-ACCTGGGGGAGTATTGCGGAGGAAGGT-(CH<sub>2</sub>)<sub>6</sub>-SH-3'; SH-cDNA<sub>2</sub>: 5'-AATACTCCCCAGGTTTTT-(CH<sub>2</sub>)<sub>6</sub>-SH-3'.

**Preparation of aptamer/nanoparticle bioconjugates:** The CdS and PbS nanoparticles were first synthesized according to a modified reported procedure.<sup>[40]</sup> In brief, AOT (14.0 g) was dissolved in a mixture of *n*-heptane (196 mL) and water (4 mL). The resulting solution was separated into two volumes of 120 and 80 mL. An aliquot of Cd(NO<sub>3</sub>)<sub>2</sub> (0.48 mL, 1.0 M) or Pb(NO<sub>3</sub>)<sub>2</sub> (0.48 mL, 1.0 M) was added to the 120 mL solution, while Na<sub>2</sub>S (0.32 mL, 1.0 M) was added to the 80 mL solution. The two solutions were stirred separately for 1 h, and then mixed under nitrogen with continuous stirring. The nanocrystals were capped with organic ligands by adding cysteamine hydrochloride (0.34 mL, 0.32 M) and sodium 2-mercaptoethane sulfonate (0.66 mL, 0.32 M) and mixing under nitrogen for 24 h. The resulting nanoparticles (CdS or PbS) were collected by removing the heptane in vacuo and washing with pyridine, hexane, acetone, and methanol.

The PbS-LBA (or CdS-ABA) bioconjugates were prepared by mixing SH-LBA (or SH-ABA, 2 μm) with a PbS (or CdS) nanoparticle suspension (1.2 mg mL<sup>-1</sup>, 500 μL) overnight at room temperature, followed by centrifugation at 10000 rpm for 45 min, removal of supernatant, and resuspension in 500 μL of 10 mM phosphate buffer (PB, 140 mM NaCl, 5 mM MgCl<sub>2</sub>, pH 7.4).

**Multiplexed assay:** The SH-cDNAs were first hybridized with their corresponding aptamers to form double-stranded DNAs (SH-cDNA<sub>1</sub>/LBA and SH-cDNA<sub>2</sub>/ABA) separately by mixing aptamers (2.4 μm) with cDNAs (2.0 μm) in the annealing buffer (10 mM Tris-HCl, 100 mM NaCl, 50 mM EDTA, pH 7.4). The mixture was heated to 95 °C for 10 min, and cooled down to 25 °C at a rate of 1 °C min<sup>-1</sup>.

The gold substrates (6 × 3 × 0.2 mm) for SH-cDNA/aptamer immobilization were cleaned with piranha solution (mixture of concentrated H<sub>2</sub>SO<sub>4</sub>/H<sub>2</sub>O<sub>2</sub> at a volume ratio of 3:1) and rinsed with ultrapure water. Next, a mixture (100 μL) of SH-cDNA<sub>1</sub>/LBA (1 μm) and SH-cDNA<sub>2</sub>/ABA (1 μm) were incubated with the gold substrates overnight (in 1.5 mL centrifuge tubes), followed by surface blocking with 6-mercapto-1-hexanol (2 mM) for 1 h. The surface-modified gold substrates were washed with PB, and the target molecules of various concentrations were added and incubated for 40 min. After washing with PB, a mixture of PbS-LBA and CdS-ABA were introduced to the tubes and incubated for 30 min. The gold substrates were then washed twice with 10 mM phosphate Tween buffer (PBT, 140 mM NaCl, 5 mM MgCl<sub>2</sub>, 0.01 % Tween 20, pH 7.4) and transferred to new tubes, and washed again with PBT.

**Dissolution of nanoparticles and EC measurements:** The gold substrates were finally treated with nitric acid (100 μL, 1.0 M) for 2 h, and the resulting solutions were added to a 1 mL EC glass cell containing 10 ppm Hg<sup>II</sup> and 900 μL of acetate buffer (0.2 M, pH 5.2). The SWV stripping detection involved a 1 min pretreatment at +0.6 V, 2 min accumulation at -1.1 V, and scanning the potential from -1.0 to -0.3 V with a potential step of 4 mV, a frequency of 25 Hz, and an amplitude of 25 mV. The data was processed with the "linear-baseline-correction" function of the CHI 852C software.

## Acknowledgements

This work is supported by National Natural Science Foundation of China (no. 20905062 and 20675064), Natural Science Foundation Project of Chongqing City (CSTC-2009BB5003), State Key Laboratory of Electroanalytical Chemistry (SKLEAC2010009), China Postdoctoral Science Foundation (20090460715 and 201003305), Fundamental Research Funds

for the Central Universities (XDJK2009B013) and research funds from Southwest University (SWUB2008078).

**Keywords:** adenosine triphosphate • aptamers • lysozymes • multiplexed detection • nanoparticles

- [1] M. Ferrari, *Nat. Rev. Cancer* **2005**, *5*, 161.
- [2] J. Trape, J. Perez de Olaguer, J. Buxo, L. Lopez, *Clin. Chem.* **2004**, *51*, 219.
- [3] J. A. Ludwig, J. N. Weinstein, *Nat. Rev. Cancer* **2005**, *5*, 845.
- [4] Z. R. Yurkovetsky, J. M. Kirkwood, H. D. Edington, A. M. Marrangoni, L. Velikokhatnaya, M. T. Winans, E. Gorelik, A. E. Lokshin, *Clin. Cancer Res.* **2007**, *13*, 2422.
- [5] B. K. Kim, J. W. Lee, P. J. Park, Y. S. Shin, W. Y. Lee, K. A. Lee, S. Ye, H. Hyun, K. N. Kang, D. Yeo, Y. Kim, S. Y. Ohn, D. Y. Noh, C. W. Kim, *Breast Cancer Res.* **2009**, *11*, R22.
- [6] M. Han, X. Gao, J. Z. Su, S. Nie, *Nat. Biotechnol.* **2001**, *19*, 631.
- [7] E. R. Goldman, A. R. Clapp, G. P. Anderson, H. T. Uyeda, J. M. Mauro, I. L. Medintz, H. Mattoussi, *Anal. Chem.* **2004**, *76*, 684.
- [8] J. Liu, J. H. Lee, Y. Lu, *Anal. Chem.* **2007**, *79*, 4120.
- [9] C. N. Allen, N. Lequeux, C. Chassenieux, G. Tessier, B. Dubertret, *Adv. Mater.* **2007**, *19*, 4420.
- [10] J. Zhang, L. Wang, H. Zhang, F. Boey, S. Song, C. Fan, *Small* **2009**, *5*, 201.
- [11] S. Rauf, A. Glidle, J. M. Cooper, *Chem. Commun.* **2010**, *46*, 2814.
- [12] J. Wang, G. Liu, A. Merkoci, *J. Am. Chem. Soc.* **2003**, *125*, 3214.
- [13] G. Liu, J. Wang, J. Kim, M. R. Jan, *Anal. Chem.* **2004**, *76*, 7126.
- [14] J. A. Hansen, J. Wang, A. N. Kawde, Y. Xiang, K. V. Gothelf, G. Collins, *J. Am. Chem. Soc.* **2006**, *128*, 2228.
- [15] I. Willner, M. Zayats, *Angew. Chem.* **2007**, *119*, 6528; *Angew. Chem. Int. Ed.* **2007**, *46*, 6408.
- [16] S. R. Nicewarner-Pena, R. G. Freeman, B. D. Reiss, L. He, D. J. Pena, I. D. Walton, R. Cromer, C. D. Keating, M. J. Natan, *Science* **2001**, *294*, 137.
- [17] J. B. H. Tok, F. Y. S. Chuang, M. C. Kao, K. A. Rose, S. S. Pannu, M. Y. Sha, G. Chakarova, S. G. Penn, G. M. Dougherty, *Angew. Chem.* **2006**, *118*, 7054; *Angew. Chem. Int. Ed.* **2006**, *45*, 6900.
- [18] M. Y. Sha, I. D. Walton, S. M. Norton, M. Taylor, M. Yamanaka, M. J. Natan, C. Xu, S. Drmanac, S. Huang, A. Borcherdig, R. Drmanac, S. G. Penn, *Anal. Bioanal. Chem.* **2006**, *384*, 658.
- [19] W. Zheng, L. He, *J. Am. Chem. Soc.* **2009**, *131*, 3432.
- [20] Y. Li, Y. T. H. Cu, D. Luo, *Nat. Biotechnol.* **2005**, *23*, 885.
- [21] X. W. Zhao, Z. B. Liu, H. Yang, K. Nagai, Y. H. Zhao, Z. Z. Gu, *Chem. Mater.* **2006**, *18*, 2443.
- [22] D. C. Pregibon, M. Toner, P. S. Doyle, *Science* **2007**, *315*, 1393.
- [23] X. Pei, B. Chen, L. Li, F. Gao, Z. Jiang, *Analyst* **2010**, *135*, 177.
- [24] Y. Long, Z. Zhang, X. Yan, J. Xing, K. Zhang, J. Huang, J. Zheng, W. Li, *Anal. Chim. Acta* **2010**, *665*, 63.
- [25] S. I. Stoeva, J. S. Lee, J. E. Smith, S. T. Rosen, C. A. Mirkin, *J. Am. Chem. Soc.* **2006**, *128*, 8378.
- [26] S. I. Stoeva, J. S. Lee, C. S. Thaxton, C. A. Mirkin, *Angew. Chem.* **2006**, *118*, 3381; *Angew. Chem. Int. Ed.* **2006**, *45*, 3303.
- [27] H. P. Huang, G. Jie, R. Cui, J. J. Zhu, *Electrochem. Commun.* **2009**, *11*, 816.
- [28] C. Deng, J. Chen, L. Nie, Z. Nie, S. Yao, *Anal. Chem.* **2009**, *81*, 9972.
- [29] Y. Peng, D. Zhang, Y. Li, H. Qi, Q. Gao, C. Zhang, *Biosens. Bioelectron.* **2009**, *25*, 94.
- [30] M. Zayats, Y. Huang, R. Gill, C. Ma, I. Willner, *J. Am. Chem. Soc.* **2006**, *128*, 13666.
- [31] Z. Tang, P. Mallikaratchy, R. Yang, Y. Kim, Z. Zhu, H. Wang, W. Tan, *J. Am. Chem. Soc.* **2008**, *130*, 11268.
- [32] C. Zhang, L. W. Johnson, *Anal. Chem.* **2009**, *81*, 3051.
- [33] J. Liu, Y. Lu, *Angew. Chem.* **2005**, *118*, 96; *Angew. Chem. Int. Ed.* **2005**, *45*, 90.
- [34] B. R. Baker, R. Y. Lai, M. S. Wood, E. H. Doctor, A. J. Heeger, K. W. Plaxco, *J. Am. Chem. Soc.* **2006**, *128*, 3138.

- [35] J. Zhang, L. Wang, D. Pan, S. Song, F. Y. Boyer, H. Zhang, C. Fan, *Small* **2008**, *4*, 1196.
- [36] D. Li, B. Shlyahovsky, J. Elbaz, I. Willner, *J. Am. Chem. Soc.* **2007**, *129*, 5804.
- [37] X. Zuo, Y. Xiao, K. W. Plaxco, *J. Am. Chem. Soc.* **2009**, *131*, 6944.
- [38] Y. Xiang, Y. Zhang, Y. Chang, Y. Chai, J. Wang, R. Yuan, *Anal. Chem.* **2010**, *82*, 1138.
- [39] J. Wang, G. Liu, G. Rivas, *Anal. Chem.* **2003**, *75*, 4667.
- [40] I. Willner, F. Patolsky, J. Wasserman, *Angew. Chem.* **2001**, *113*, 1913; *Angew. Chem. Int. Ed.* **2001**, *40*, 1861.

Received: September 6, 2010  
Published online: November 24, 2010